

A SUGGESTED ANALYTICAL SOLUTION OF ORTHOTROPIC COMPOSITE PLATE STRUCTURE WITH CRACK EFFECT

¹MUHSIN J. JWEEG, ²ALI S. HAMMOOD & ²MUHANNAD AL-WAILY

¹Al-Nahrain University, College of Engineering, Mechanical Engineering Department, Baghdad, Iraq

²Kufa University, College of Engineering, Material Engineering Department, Najaf, Iraq

ABSTRACT

The existence of a defect like a crack will lead to change in natural frequency of the plate and enlargement of the crack will also lead another change in natural frequency with the change of the size or position of the crack. So this study focuses on finding the natural frequency for orthotropic composite plates with crack considering the size of the crack (crack length and depth through plate thickness) an crack position in the plate in x, y directions, also slant of the crack. The natural frequency is studied for composite material strengthen by long, and woven fibers with the effect of crack size and position, plate thickness, aspect ratio, the type of plate fixing where three type of fixing used (SSSS, SSCC, SSFF).

Two methods are used to find the natural frequency of composite plate: First method is supposed analytical solution to solve the equation of motion considering the effect of size, and position crack on the natural frequency of the composite plate. Second method is finite element solution using ANSYS (ver. 14) program. A comparison made between the two methods and the error percentage is not exceeds of 3.5%.

The results shows that the natural frequency decreases as crack size (length or width) increases. The natural frequency decreases when the crack in the middle of the plate over any position of the crack. The effect of crack when it reaches the middle is higher than when it's in the other places. The natural frequency is decreases as plate width increases, (aspect ratio and plate thickness).

KEYWORDS: Plate Vibration, Crack Study, Composite Plate with Crack Effect, Crack Plate Vibration

INTRODUCTION

Damage detection of one-dimensional structures by vibration analysis, is a new technique in non-destructive evaluation methods. The conventional nondestructive testing methods unlike the vibration analysis methods are expensive and time-consuming. Several researchers have worked on the influence of cracks on the natural frequencies and mode shapes of structures, **S. E. Khadem and M. Rezaee (2000-b)**.

All efforts to predict crack growth and fatigue in a composite laminate are affected by the unique and complex manner in which cracks can grow in a laminate. Cracks tend to grow in the matrix parallel to the fibers. Thus, if a crack is cut parallel to the fibers, it will grow in a direction parallel to itself, i.e., in a self-similar manner. However, if a crack is cut at some angle to the fibers, then the crack will still grow parallel to the fibers and not parallel to itself, i.e., non-self-similar crack growth. Then, because a composite laminate has many layers at various orientations, a crack cut in a laminate results in crack growth that is locally sometimes self-similar and sometimes not. Globally, crack growth is non-self-similar, so predicting the effects of many kinds of damage growth is very difficult, if not impossible, **R. M. Jones (1999)**.

In 2000 S. E. Khadem and M. Rezaee-a, introduced a new functions named 'modified comparison functions' and used for vibration analysis of a simply supported rectangular cracked plate. It is assumed that the crack having an arbitrary

length, depth and location is parallel to one side of the plate. Elastic behavior of the plate at crack location is considered as a line spring with a varying stiffness along the crack.

Also in same year **S. E. Khadem and M. Rezaee-b**, established an analytical approach to the crack detection of rectangular plates under uniform external loads by vibration analysis. The damage is considered as an all-over part-through crack parallel to one edge of the plate. Avoiding non-linearity, it is assumed that the crack, at all dynamical conditions, is open.

S. S. Kessler et al. 2001, presented part of an experimental and analytical survey of candidate methods for in-situ damage detection of composite materials. Experimental results are presented for the application of Lamb wave techniques to quasi-isotropic graphite-epoxy thin coupons and sandwich beams containing representative damage modes, including delamination, transverse ply cracks and through-holes.

Also in 2004 **L. Wang**, presented an exact solutions of dispersive relations in a composite lamina and composite laminate are first deduced from three-dimensional (3-D) elasticity theory. The dispersion relations containing infinite number of symmetric and anti-symmetric wave modes are numerically solved. Then, to make dispersive wave solutions tractable in composites, a higher-order plate theory is proposed.

And in 2008 **A. Israr (2008)**, concerned with analytical modelling of the effects of cracks in structural plates and panels within aerospace systems such as aeroplane fuselage, wing, and tail-plane structures, and, as such, is part of a larger body of research into damage detection methodologies in such systems. This study is based on generating a so-called reduced order analytical model of the behaviour of the plate panel, within which a crack with some arbitrary characteristics is present, and which is subjected to a force that causes it to vibrate.

In this study, a suggested analytical solution to driving the equation of motion for a given set of boundary conditions governing the vibrations of orthotropic composite plate with crack effect. In addition to study the effect of all crack parameters and plate geometry on the natural frequency for different types of composite plate.

Theoretical Study

To model a crack with a finite length in a cracked rectangular plate, a rectangular plate may be considered as shown in **Fig. 1**; the crack is $2c$ in length and runs parallel with one side of the plate.

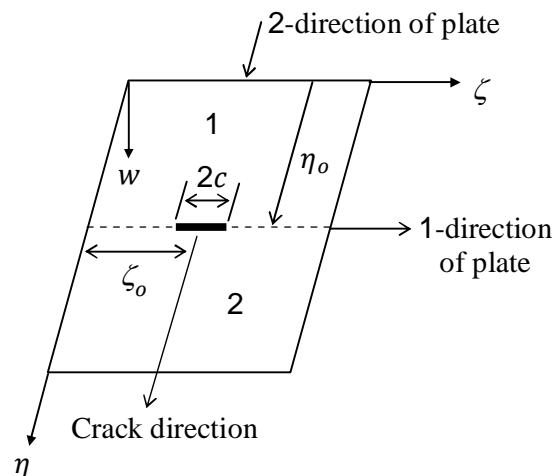


Fig. 1: Orthotropic Plate with Crack

The coordinates of the crack center are represented by x_o and y_o . Using non-dimensional parameters as, **S. E. Khadem and M. Rezaee (2000-a)**,

$$2c = \frac{2C}{a} \quad \text{crack relative length}$$

$$\xi = \frac{h_o}{H} \quad \text{crack relative depth at its center}$$

$$\begin{aligned} \zeta_o &= \frac{x_o}{a} \\ \eta_o &= \frac{y_o}{b} \end{aligned} \quad \text{crack center - coordinates} \quad (1)$$

Where, a , b and H represent dimensions of the plate in x , y and z directions, respectively, and h_o represents the crack depth at its center.

When the plate is only subjected to the bending moments, the Formula or nominal bending stress at the location of the crack with a finite length becomes,

$$\sigma_b^o = \frac{\sigma_{b_o}}{1 + \left[3(3 + \nu_{21})(1 - \nu_{21}) \frac{\alpha_{bb}^o}{(2c/H)} \right]} \quad (2)$$

Where, σ_b^o is the nominal bending stress at the crack location and on the surface of the plate, at the crack direction, σ_{b_o} is the nominal bending stress at the location of the crack with an infinite length and on the surface of the plate equal to stress in 2-direction of orthotropic plate (σ_2), at the crack direction, α_{bb}^o is the non-dimensional bending compliance coefficient at the crack center, and, ν is the Poisson ratio.

If the shape of the crack is considered as a semi-ellipse, in Cartesian coordinate system, then the function representing the shape of the crack will be, **S. E. Khadem and M. Rezaee (2000-a)**,

$$h(x) = \begin{cases} 0 & , \text{for } 0 < x < (x_o - C) \\ h_o \left[1 - \left(\frac{x - x_o}{C} \right)^2 \right]^{1/2} & , \text{for } (x_o - C) < x < (x_o + C) \\ 0 & , \text{for } (x_o + C) < x < a \end{cases} \quad (3)$$

For vibration analysis of the plate having a crack with a finite length, relation Eq. (3) can be expanded as a sum of sine and cosine functions in the domain $0 \leq x \leq a$ by Fourier series.

However, the application of this method may be inefficient due to time consuming and intensive computational effects. Therefore, by using the following equation, **S. E. Khadem and M. Rezaee (2000-a)**,

$$\alpha_{bb} = \frac{1}{H} \int_0^h g_b^2 dh \quad (4)$$

Where, g_b is the dimensionless function of the relative crack depth, And is defined as, **S. E. Khadem and M. Rezaee (2000-b)**,

$$g_b = \xi^{1/2} [1.99 - 2.47 \xi + 12.97 \xi^2 - 23.17 \xi^3 + 24.80 \xi^4] \quad (5)$$

The method for the choice of α_{bb}^o suggest to identify α_{bb}^o with the value of α_{bb} at $x = x_o$ (*center of crack*), **J. R. Rice and N. Levy (1972)**.

A function representing dimensionless bending compliance coefficient is directly suggested as a function of dimensionless coordinate, ζ , which is free of the above-mentioned difficulties, as follows, **S. E. Khadem and M. Rezaee (2000-a)**,

$$\alpha_{bb}(\zeta) = \alpha_{bb}^0 e^{-[(\zeta-\zeta_0) e]^2/(2c)^2} \quad (6)$$

One may suggest the variation of the nominal bending stress on the hypothetical boundary as the following new function, **S. E. Khadem and M. Rezaee (2000-a)**,

$$\sigma_b(\zeta) = \sigma_{b_{\infty}} - (\sigma_{b_{\infty}} - \sigma_b^0) f(\zeta) \quad (7)$$

Where $f(\zeta)$ is the 'crack shape function' and is defined as,

$$f(\zeta) = e^{-[(\zeta-\zeta_0) e]^2/(2c)^2} \quad (8)$$

On the other hand, the slope discontinuity at both sides of the crack location due to bending moments is proportional to bending compliance of the crack and nominal bending stress, and is given by, **S. E. Khadem and M. Rezaee (2000-a)**,

$$\theta_{slop}(\zeta) = \frac{12(1-\nu_{21}^2)}{E} \sigma_b \alpha_{bb} \quad (9)$$

The governing equation for the free vibration of a rectangular isotropic plate is given by, **S. E. Khadem and M. Rezaee (2000-a)**,

$$D \nabla^4 w + \bar{m} \frac{\partial^2 w}{\partial t^2} = 0 \quad (10)$$

Where, $w = w(x, y, t)$, ∇ is the biharmonic operator, \bar{m} is the mass per unit area of the plate, D is the plate flexural rigidity $= \frac{E H^3}{12(1-\nu^2)}$.

Using the separation of variables technique to solving Eq. (4.25), as,

$$w(x, y, t) = W(x, y) \cdot T(t) \quad (11)$$

Then,

$$\ddot{T} + \omega^2 T = 0, \text{ and, } \nabla^4 W - \omega^2 \frac{\bar{m}}{D} W = 0 \quad (12)$$

Transformation Eq. (12) in terms of dimensionless co-ordinates ζ and η as, $\zeta = \frac{x}{a}$, $\eta = \frac{y}{b}$. Then,

$$\phi^4 \frac{\partial^4 W}{\partial \zeta^4} + 2\phi^2 \frac{\partial^4 W}{\partial \zeta^2 \partial \eta^2} + \frac{\partial^4 W}{\partial \eta^4} - \lambda^4 W = 0 \quad (13)$$

Where, $\lambda^4 = \omega^2 \frac{\bar{m}}{D} b^4$, $\phi = \frac{b}{a}$

To solving Eq. (4.31) using boundary as simply supported along the edges $\zeta = 0$ and 1, and arbitrary edge condition at $\eta = 0$ and 1, the solution of Eq. (4.31) may be expressed in the form, **A. C. Ugural (1999)**,

$$W(\zeta, \eta) = \sum_{m=1}^{\infty} Y_m(\eta) \sin(m \pi \zeta) \quad (14)$$

By substitution Eq. (14) into Eq. (13), get,

$$\frac{d^4 Y}{d\eta^4} - 2[m \pi \phi]^2 \frac{d^2 Y}{d\eta^2} + [(m \pi \phi)^4 - \lambda^4] Y = 0 \quad (15)$$

To solving Eq. (15) using of linear differential operators, **H. Anton et. al. (2002)**, get, for $\lambda^2 > (m \pi \phi)^2$,

$$Y_m(\eta) = A_m \cosh(\beta_m \eta) + B_m \sinh(\beta_m \eta) + C_m \cos(\gamma_m \eta) + D_m \sin(\gamma_m \eta) \quad (16)$$

Where, $\beta_m = \sqrt{((m \pi \phi)^2 + \lambda^2)}$,

$\gamma_m = \sqrt{(\lambda^2 - (m \pi \phi)^2)}$.

By applying Eq. (4.33) to two regions of the cracked plate shown in **Fig. 1**, one may require eight boundary conditions. The boundary conditions are applied to regions (1) and (2), respectively, at $\eta = 0$ and 1, and to a hypothetical boundary separating the two regions. Because of the form of the plate supports at two edges simply support, the boundary conditions at $\zeta = 0$ and 1 for two regions are satisfied by Eq. (14), **S. E. Khadem and M. Rezaee (2000-a)**. Then, Eq. (14) for two regions become,

$$W_1(\zeta, \eta) = \begin{bmatrix} A_{m_1} \cosh(\beta_m \eta) + \\ B_{m_1} \sinh(\beta_m \eta) + \\ C_{m_1} \cos(\gamma_m \eta) + \\ D_{m_1} \sin(\gamma_m \eta) \end{bmatrix} \sin(m \pi \zeta)$$

for $(\eta = 0 \rightarrow \eta_o)$

$$W_2(\zeta, \eta) = \begin{bmatrix} A_{m_2} \cosh(\beta_m \eta) + \\ B_{m_2} \sinh(\beta_m \eta) + \\ C_{m_2} \cos(\gamma_m \eta) + \\ D_{m_2} \sin(\gamma_m \eta) \end{bmatrix} \sin(m \pi \zeta)$$

for $(\eta = \eta_o \rightarrow 1)$

(17)

The boundary conditions along the crack at $\eta = \eta_o$ are, **S. E. Khadem and M. Rezaee (2000-a)**,

$$W_1(\zeta, \eta)|_{\eta_o} = W_2(\zeta, \eta)|_{\eta_o}, M_{1\eta} = M_{2\eta} \Rightarrow \frac{\partial^2 W_1}{\partial \eta^2} + \nu \phi^2 \frac{\partial^2 W_1}{\partial \zeta^2} \Big|_{\eta_o} = \frac{\partial^2 W_2}{\partial \eta^2} + \nu \phi^2 \frac{\partial^2 W_2}{\partial \zeta^2} \Big|_{\eta_o}$$

$$V_{1\eta} = V_{2\eta} \Rightarrow \frac{\partial^3 W_1}{\partial \eta^3} + (2 - \nu) \phi^2 \frac{\partial^3 W_1}{\partial \zeta^2 \partial \eta} \Big|_{\eta_o} = \frac{\partial^3 W_2}{\partial \eta^3} + (2 - \nu) \phi^2 \frac{\partial^3 W_2}{\partial \zeta^2 \partial \eta} \Big|_{\eta_o}$$

$$\frac{\partial W_1}{\partial \eta} - \theta_{stop}(\zeta) - \frac{\partial W_2}{\partial \eta} \Big|_{\eta_o} = 0 \quad (18)$$

For using, **A. C. Ugural (1999)**,

$$\sigma_{b_x} = -\frac{E H}{2 b^2 (1 - \nu^2)} \left(\frac{\partial^2 W}{\partial \eta^2} + \nu \phi^2 \frac{\partial^2 W}{\partial \zeta^2} \right)$$

$$\text{Then, } \theta_{stop}(\zeta) = f_e(\zeta) \left(\frac{\partial^2 W}{\partial \eta^2} + \nu \phi^2 \frac{\partial^2 W}{\partial \zeta^2} \right)$$

Then, fourth boundary condition in Eq. (18), become,

$$\frac{\partial W_1}{\partial \eta} - f_e(\zeta) \left(\frac{\partial^2 W_1}{\partial \eta^2} + \nu \phi^2 \frac{\partial^2 W_1}{\partial \zeta^2} \right) - \frac{\partial W_2}{\partial \eta} \Big|_{\eta_o} = 0$$

The boundary conditions at $\eta = 0$ and 1, for regions (1) and (2), respectively, **A. C. Ugural (1999)**, are,

➤ **Simply Supported Edges,**

At the simply support considered, the deflection and bending moment are both zero. Hence,

$$\begin{aligned}
W_1(\zeta, \eta)|_{\eta=0} = 0, \quad \frac{\partial^2 W_1}{\partial \eta^2} + \nu \phi^2 \frac{\partial^2 W_1}{\partial \zeta^2} \Big|_{\eta=0} &= 0 \\
W_2(\zeta, \eta)|_{\eta=1} = 0, \quad \frac{\partial^2 W_2}{\partial \eta^2} + \nu \phi^2 \frac{\partial^2 W_2}{\partial \zeta^2} \Big|_{\eta=1} &= 0
\end{aligned} \tag{19}$$

➤ **Clamped Supported Edges,**

In this case both the deflection and slope must vanish. That is,

$$\begin{aligned}
W_1(\zeta, \eta)|_{\eta=0} = 0, \quad \frac{\partial W_1}{\partial \eta} \Big|_{\eta=0} &= 0, \\
W_2(\zeta, \eta)|_{\eta=1} = 0, \quad \frac{\partial W_2}{\partial \eta} \Big|_{\eta=1} &= 0
\end{aligned} \tag{20}$$

➤ **Free Supported Edges,**

In this case both bending moment and vertical shear force zero. Hence,

$$\begin{aligned}
\frac{\partial^2 W_1}{\partial \eta^2} + \nu \phi^2 \frac{\partial^2 W_1}{\partial \zeta^2} \Big|_{\eta=0} &= 0 \\
\frac{\partial^3 W_1}{\partial \eta^3} + (2 - \nu) \phi^2 \frac{\partial^3 W_1}{\partial \zeta^2 \partial \eta} \Big|_{\eta=0} &= 0 \\
\frac{\partial^2 W_2}{\partial \eta^2} + \nu \phi^2 \frac{\partial^2 W_2}{\partial \zeta^2} \Big|_{\eta=1} &= 0 \\
\frac{\partial^3 W_2}{\partial \eta^3} + (2 - \nu) \phi^2 \frac{\partial^3 W_2}{\partial \zeta^2 \partial \eta} \Big|_{\eta=1} &= 0
\end{aligned} \tag{21}$$

By using boundary conditions in Eqs. (19) to (21) for each case and boundary conditions along the crack, in Eq. (18), get the general solution of Eq. (17), For $\lambda^2 > (m \pi \phi)^2$, as,

➤ **Simply Supported Edges,**

By substitution boundary conditions in Eqs. (19) and (18) into Eq. (17), get,

$$\begin{aligned}
W_1(\zeta, \eta) &= B_{m_1} \begin{bmatrix} f_1(\zeta) \sinh(\beta_m \eta) + \\ f_2(\zeta) \sin(\gamma_m \eta) \end{bmatrix} \\
&\quad (\eta = 0 \rightarrow \eta_o) \\
W_2(\zeta, \eta) &= B_{m_1} \begin{bmatrix} f_3(\zeta) (\sinh(\beta_m \eta) - \tanh \beta_m \cosh(\beta_m \eta)) + \\ f_4(\zeta) (\sin(\gamma_m \eta) - \tan \gamma_m \cos(\gamma_m \eta)) \end{bmatrix} \\
&\quad (\eta = \eta_o \rightarrow 1)
\end{aligned} \tag{22}$$

Where,

$$\begin{aligned}
f_1(\zeta) &= \sin(m \pi \zeta), \quad f_2(\zeta) = S_1 \sin(m \pi \zeta) \\
f_3(\zeta) &= S_2 \sin(m \pi \zeta), \quad f_4(\zeta) = S_3 \sin(m \pi \zeta)
\end{aligned}$$

$$\text{For, } S_1 = \frac{\begin{bmatrix} (e_9 e_{16} - e_{12} e_{13})(e_4 e_7 - e_3 e_8) - \\ (e_1 e_8 - e_5 e_4)(e_{12} e_{15} - e_{11} e_{16}) \end{bmatrix}}{\begin{bmatrix} (e_2 e_8 - e_6 e_4)(e_{12} e_{15} - e_{11} e_{16}) - \\ (e_{10} e_{16} - e_{12} e_{14})(e_4 e_7 - e_3 e_8) \end{bmatrix}}$$

$$S_2 = \frac{\begin{bmatrix} (e_9 e_{14} - e_{10} e_{13})(e_8 e_2 - e_4 e_6) - \\ (e_1 e_6 - e_5 e_2)(e_{16} e_{10} - e_{12} e_{14}) \end{bmatrix}}{\begin{bmatrix} (e_3 e_6 - e_7 e_2)(e_{16} e_{10} - e_{12} e_{14}) - \\ (e_{11} e_{14} - e_{10} e_{15})(e_8 e_2 - e_4 e_6) \end{bmatrix}}$$

$$S_3 = \frac{\begin{bmatrix} (e_9 e_{15} - e_{11} e_{13})(e_6 e_3 - e_2 e_7) - \\ (e_1 e_7 - e_5 e_3)(e_{14} e_{11} - e_{10} e_{15}) \end{bmatrix}}{\begin{bmatrix} (e_4 e_7 - e_3 e_8)(e_{14} e_{11} - e_{10} e_{15}) - \\ (e_{12} e_{15} - e_{11} e_{16})(e_6 e_3 - e_2 e_7) \end{bmatrix}}$$

For,

$$e_1 = \sinh(\beta_m \eta_o), e_2 = \sin(\gamma_m \eta_o),$$

$$e_3 = -\left(\frac{\sinh(\beta_m \eta_o)}{\tanh \beta_m \cosh(\beta_m \eta_o)} \right)$$

$$e_4 = -(\sin(\gamma_m \eta_o) - \tan \gamma_m \cos(\gamma_m \eta_o)), e_5 = \sinh(\beta_m \eta_o) (\beta_m^2 - (m \pi)^2 \nu \phi^2),$$

$$e_6 = -\sin(\gamma_m \eta_o) (\gamma_m^2 + (m \pi)^2 \nu \phi^2)$$

$$e_7 = -\left(\frac{\sinh(\beta_m \eta_o)}{\tanh \beta_m \cosh(\beta_m \eta_o)} \right) (\beta_m^2 - (m \pi)^2 \nu \phi^2)$$

$$e_8 = (\sin(\gamma_m \eta_o) - \tan \gamma_m \cos(\gamma_m \eta_o)) (\gamma_m^2 + (m \pi)^2 \nu \phi^2)$$

$$e_9 = \cosh(\beta_m \eta_o) (\beta_m^3 - (m \pi)^2 (2 - \nu) \phi^2 \beta_m)$$

$$e_{10} = -\cos(\gamma_m \eta_o) (\gamma_m^3 + (m \pi)^2 (2 - \nu) \phi^2 \gamma_m)$$

$$e_{11} = -\left(\frac{\cosh(\beta_m \eta_o)}{\tanh \beta_m \sinh(\beta_m \eta_o)} \right) (\beta_m^3 - (m \pi)^2 (2 - \nu) \phi^2 \beta_m)$$

$$e_{12} = (\cos(\gamma_m \eta_o) + \tan \gamma_m \sin(\gamma_m \eta_o)) (\gamma_m^3 + (m \pi)^2 (2 - \nu) \phi^2 \gamma_m)$$

$$e_{13} = [\beta_m \cosh(\beta_m \eta_o) - f_e(\zeta) \sinh(\beta_m \eta_o) (\beta_m^2 - (m \pi)^2 \nu \phi^2)]$$

$$e_{14} = [\gamma_m \cos(\gamma_m \eta_o) + f_e(\zeta) \sin(\gamma_m \eta_o) (\gamma_m^2 + (m \pi)^2 \nu \phi^2)]$$

$$e_{15} = -\beta_m (\cosh(\beta_m \eta_o) - \tanh \beta_m \sinh(\beta_m \eta_o))$$

$$e_{16} = -\gamma_m (\cos(\gamma_m \eta_o) + \tan \gamma_m \sin(\gamma_m \eta_o))$$

And the value of λ can be evaluated from the characteristics equations, as,

$$\begin{vmatrix} e_1 & e_2 & e_3 & e_4 \\ e_5 & e_6 & e_7 & e_8 \\ e_9 & e_{10} & e_{11} & e_{12} \\ e_{13} & e_{14} & e_{15} & e_{16} \end{vmatrix} = 0 \quad (23)$$

➤ **Clamped Supported Edges,**

By substitution boundary conditions in Eqs. (20) and (18) into Eq. (17), get,

$$W_1(\zeta, \eta) = B_{m_1} \begin{bmatrix} f_1(\zeta) \left(\sinh(\beta_m \eta) - \frac{\beta_m}{\gamma_m} \sin(\gamma_m \eta) \right) + \\ f_2(\zeta) (\cos(\gamma_m \eta) - \cosh(\beta_m \eta)) \end{bmatrix}$$

$$(\eta = 0 \rightarrow \eta_o)$$

$$W_2(\zeta, \eta) = B_{m_1} \left[\begin{array}{c} f_3(\zeta) \left(\begin{array}{c} \sinh(\beta_m \eta) + d_4 \cosh(\beta_m \eta) + \\ d_2 \sin(\gamma_m \eta) \end{array} \right) + \\ f_4(\zeta) \left(\begin{array}{c} \cos(\gamma_m \eta) + d_3 \cosh(\beta_m \eta) + \\ d_1 \sin(\gamma_m \eta) \end{array} \right) \end{array} \right] \quad (\eta = \eta_o \rightarrow 1) \quad (24)$$

Where,

$$f_1(\zeta) = \sin(m \pi \zeta), f_2(\zeta) = \bar{S}_1 \sin(m \pi \zeta)$$

$$f_3(\zeta) = \bar{S}_2 \sin(m \pi \zeta), f_4(\zeta) = \bar{S}_3 \sin(m \pi \zeta)$$

$$\text{And, } d_1 = \frac{(\tan \gamma_m + \frac{\beta_m}{\gamma_m} \tanh \beta_m)}{(1 - \frac{\beta_m}{\gamma_m} \tanh \beta_m \tan \gamma_m)},$$

$$d_2 = \frac{\beta_m (\tanh \beta_m \sinh \beta_m - \cosh \beta_m)}{\gamma_m (\cos \gamma_m - \frac{\beta_m}{\gamma_m} \tanh \beta_m \sin \gamma_m)}$$

$$d_3 = -\frac{(\tan \gamma_m \sin \gamma_m + \cos \gamma_m)}{(\cosh \beta_m - \frac{\beta_m}{\gamma_m} \tan \gamma_m \sinh \beta_m)},$$

$$d_4 = \frac{(\frac{\beta_m}{\gamma_m} \tan \gamma_m - \tanh \beta_m)}{(1 - \frac{\beta_m}{\gamma_m} \tanh \beta_m \tan \gamma_m)}$$

$$\text{For, } \bar{S}_1 = \frac{[(\bar{e}_9 \bar{e}_{16} - \bar{e}_{12} \bar{e}_{13})(\bar{e}_4 \bar{e}_7 - \bar{e}_3 \bar{e}_8) - (\bar{e}_1 \bar{e}_8 - \bar{e}_5 \bar{e}_4)(\bar{e}_{12} \bar{e}_{15} - \bar{e}_{11} \bar{e}_{16})]}{[(\bar{e}_2 \bar{e}_8 - \bar{e}_6 \bar{e}_4)(\bar{e}_{12} \bar{e}_{15} - \bar{e}_{11} \bar{e}_{16}) - (\bar{e}_{10} \bar{e}_{16} - \bar{e}_{12} \bar{e}_{14})(\bar{e}_4 \bar{e}_7 - \bar{e}_3 \bar{e}_8)]}$$

$$\bar{S}_2 = \frac{[(\bar{e}_9 \bar{e}_{14} - \bar{e}_{10} \bar{e}_{13})(\bar{e}_8 \bar{e}_2 - \bar{e}_4 \bar{e}_6) - (\bar{e}_1 \bar{e}_6 - \bar{e}_5 \bar{e}_2)(\bar{e}_{16} \bar{e}_{10} - \bar{e}_{12} \bar{e}_{14})]}{[(\bar{e}_3 \bar{e}_6 - \bar{e}_7 \bar{e}_2)(\bar{e}_{16} \bar{e}_{10} - \bar{e}_{12} \bar{e}_{14}) - (\bar{e}_{11} \bar{e}_{14} - \bar{e}_{10} \bar{e}_{15})(\bar{e}_8 \bar{e}_2 - \bar{e}_4 \bar{e}_6)]}$$

$$\bar{S}_3 = \frac{[(\bar{e}_9 \bar{e}_{15} - \bar{e}_{11} \bar{e}_{13})(\bar{e}_6 \bar{e}_3 - \bar{e}_2 \bar{e}_7) - (\bar{e}_1 \bar{e}_7 - \bar{e}_5 \bar{e}_3)(\bar{e}_{14} \bar{e}_{11} - \bar{e}_{10} \bar{e}_{15})]}{[(\bar{e}_4 \bar{e}_7 - \bar{e}_3 \bar{e}_8)(\bar{e}_{14} \bar{e}_{11} - \bar{e}_{10} \bar{e}_{15}) - (\bar{e}_{12} \bar{e}_{15} - \bar{e}_{11} \bar{e}_{16})(\bar{e}_6 \bar{e}_3 - \bar{e}_2 \bar{e}_7)]}$$

$$\text{For, } \bar{e}_1 = (\sinh(\beta_m \eta_o) - \frac{\beta_m}{\gamma_m} \sin(\gamma_m \eta_o)), \bar{e}_2 = (\cos(\gamma_m \eta_o) - \cosh(\beta_m \eta_o))$$

$$\bar{e}_3 = -(\sinh(\beta_m \eta_o) + d_4 \cosh(\beta_m \eta_o) + d_2 \sin(\gamma_m \eta_o))$$

$$\bar{e}_4 = -(\cos(\gamma_m \eta_o) + d_3 \cosh(\beta_m \eta_o) + d_1 \sin(\gamma_m \eta_o))$$

$$\bar{e}_5 = \left[\begin{array}{c} \sinh(\beta_m \eta_o) (\beta_m^2 - (m \pi)^2 \nu \phi^2) + \\ \sin(\gamma_m \eta_o) (\beta_m \gamma_m + (m \pi)^2 \nu \phi^2 \frac{\beta_m}{\gamma_m}) \end{array} \right]$$

$$\bar{e}_6 = - \left[\begin{array}{c} \cosh(\beta_m \eta_o) (\beta_m^2 - (m \pi)^2 \nu \phi^2) + \\ \cos(\gamma_m \eta_o) (\gamma_m^2 + (m \pi)^2 \nu \phi^2) \end{array} \right]$$

$$\bar{e}_7 = - \left[\begin{array}{c} (\sinh(\beta_m \eta_o) + d_4 \cosh(\beta_m \eta_o)) (\beta_m^2 - (m \pi)^2 \nu \phi^2) - \\ d_2 \sin(\gamma_m \eta_o) (\gamma_m^2 + (m \pi)^2 \nu \phi^2) \end{array} \right]$$

$$\bar{e}_8 = \left[\begin{array}{c} (\cos(\gamma_m \eta_o) + d_1 \sin(\gamma_m \eta_o)) (\gamma_m^2 + (m \pi)^2 \nu \phi^2) - \\ d_3 \cosh(\beta_m \eta_o) (\beta_m^2 - (m \pi)^2 \nu \phi^2) \end{array} \right]$$

$$\begin{aligned} \bar{e}_9 &= \left[\frac{\cosh(\beta_m \eta_o) (\beta_m^3 - (2 - \nu) \phi^2 (m \pi)^2 \beta_m) +}{\gamma_m \cos(\gamma_m \eta_o) (\gamma_m^3 + (2 - \nu) \phi^2 (m \pi)^2 \gamma_m)} \right] \\ \bar{e}_{10} &= \left[\frac{\sin(\gamma_m \eta_o) (\gamma_m^3 + (2 - \nu) \phi^2 (m \pi)^2 \gamma_m) -}{\sinh(\beta_m \eta_o) (\beta_m^3 - (2 - \nu) \phi^2 (m \pi)^2 \beta_m)} \right] \\ \bar{e}_{11} &= - \left[\frac{(\cosh(\beta_m \eta_o) +)}{d_4 \sinh(\beta_m \eta_o)} (\beta_m^3 - (2 - \nu) \phi^2 (m \pi)^2 \beta_m) - \right. \\ &\quad \left. d_2 \cos(\gamma_m \eta_o) (\gamma_m^3 + (2 - \nu) \phi^2 (m \pi)^2 \gamma_m) \right] \\ \bar{e}_{12} &= - \left[\frac{(\sin(\gamma_m \eta_o) -)}{d_1 \cos(\gamma_m \eta_o)} (\gamma_m^3 + (2 - \nu) \phi^2 (m \pi)^2 \gamma_m) + \right. \\ &\quad \left. d_3 \sinh(\beta_m \eta_o) (\beta_m^3 - (2 - \nu) \phi^2 (m \pi)^2 \beta_m) \right] \\ \bar{e}_{13} &= \left[f_e(\zeta) \left(\frac{\beta_m \cosh(\beta_m \eta_o) - \beta_m \cos(\gamma_m \eta_o) -}{\sinh(\beta_m \eta_o) (\beta_m^2 - (m \pi)^2 \nu \phi^2) +} \right. \right. \\ &\quad \left. \left. \sin(\gamma_m \eta_o) (\beta_m \gamma_m + (m \pi)^2 \nu \phi^2 \frac{\beta_m}{\gamma_m}) \right) \right] \\ \bar{e}_{14} &= - \left[f_e(\zeta) \left(\frac{\gamma_m \sin(\gamma_m \eta_o) + \beta_m \sinh(\beta_m \eta_o) -}{\cosh(\beta_m \eta_o) (\beta_m^2 - (m \pi)^2 \nu \phi^2) +} \right. \right. \\ &\quad \left. \left. \cos(\gamma_m \eta_o) (\gamma_m^2 + (m \pi)^2 \nu \phi^2) \right) \right] \\ \bar{e}_{15} &= -[\beta_m \cosh(\beta_m \eta_o) + \beta_m d_4 \sinh(\beta_m \eta_o) + \gamma_m d_2 \cos(\gamma_m \eta_o)] \\ \bar{e}_{16} &= -[\beta_m d_3 \sinh(\beta_m \eta_o) + \gamma_m d_1 \cos(\gamma_m \eta_o) - \gamma_m \sin(\gamma_m \eta_o)] \end{aligned}$$

And the value of λ can be evaluated from the characteristics equations, as,

$$\begin{vmatrix} \bar{e}_1 & \bar{e}_2 & \bar{e}_3 & \bar{e}_4 \\ \bar{e}_5 & \bar{e}_6 & \bar{e}_7 & \bar{e}_8 \\ \bar{e}_9 & \bar{e}_{10} & \bar{e}_{11} & \bar{e}_{12} \\ \bar{e}_{13} & \bar{e}_{14} & \bar{e}_{15} & \bar{e}_{16} \end{vmatrix} = 0 \quad (25)$$

➤ Free Supported Edges

By substitution boundary conditions in Eqs. (21) and (18) into Eq. (17), get,

$$\begin{aligned} W_1(\zeta, \eta) &= B_{m_1} \left[\begin{array}{l} f_1(\zeta) \left(\frac{\sinh(\beta_m \eta) +}{(\beta_m^3 - (m \pi)^2 (2 - \nu) \phi^2 \beta_m)} \sin(\gamma_m \eta) \right) + \\ f_2(\zeta) \left(\frac{\cos(\gamma_m \eta) +}{(\gamma_m^2 + (m \pi)^2 \nu \phi^2)} \cosh(\beta_m \eta) \right) \end{array} \right] \\ &\quad (\eta = 0 \rightarrow \eta_o) \\ W_2(\zeta, \eta) &= B_{m_1} \left[\begin{array}{l} f_3(\zeta) \left(\frac{\sinh(\beta_m \eta) +}{\bar{d}_{11} \cosh(\beta_m \eta) + \bar{d}_9 \sin(\gamma_m \eta)} \right) + \\ f_4(\zeta) \left(\frac{\cos(\gamma_m \eta) +}{\bar{d}_{12} \cosh(\beta_m \eta) + \bar{d}_{10} \sin(\gamma_m \eta)} \right) \end{array} \right] \\ &\quad (\eta = \eta_o \rightarrow 1) \end{aligned} \quad (26)$$

$$f_1(\zeta) = \sin(m \pi \zeta), f_2(\zeta) = \bar{\bar{S}}_1 \sin(m \pi \zeta)$$

$$f_3(\zeta) = \bar{\bar{S}}_2 \sin(m \pi \zeta), f_4(\zeta) = \bar{\bar{S}}_3 \sin(m \pi \zeta)$$

$$\text{And, } \bar{d}_9 = \frac{(\bar{d}_5 \bar{d}_2 - \bar{d}_6 \bar{d}_1)}{(\bar{d}_8 \bar{d}_1 - \bar{d}_4 \bar{d}_5)}, \bar{d}_{10} = \frac{(\bar{d}_5 \bar{d}_3 - \bar{d}_7 \bar{d}_1)}{(\bar{d}_8 \bar{d}_1 - \bar{d}_4 \bar{d}_5)}, \bar{d}_{11} = -\left(\bar{d}_9 \frac{\bar{d}_4}{\bar{d}_1} + \frac{\bar{d}_2}{\bar{d}_1}\right), \bar{d}_{12} = -\left(\bar{d}_{10} \frac{\bar{d}_4}{\bar{d}_1} + \frac{\bar{d}_3}{\bar{d}_1}\right)$$

$$\text{For, } \bar{d}_1 = \cosh \beta_m (\beta_m^2 - (m \pi)^2 \nu \phi^2),$$

$$\bar{d}_2 = \sinh \beta_m (\beta_m^2 - (m \pi)^2 \nu \phi^2)$$

$$\bar{d}_3 = -\cos \gamma_m (\gamma_m^2 + (m \pi)^2 \nu \phi^2),$$

$$\bar{d}_4 = -\sin \gamma_m (\gamma_m^2 + (m \pi)^2 \nu \phi^2)$$

$$\bar{d}_5 = \sinh \beta_m (\beta_m^3 - (m \pi)^2 (2 - \nu) \phi^2 \beta_m), \bar{d}_6 = \cosh \beta_m (\beta_m^3 - (m \pi)^2 (2 - \nu) \phi^2 \beta_m)$$

$$\bar{d}_7 = \sin \gamma_m (\gamma_m^3 + (m \pi)^2 (2 - \nu) \phi^2 \gamma_m), \bar{d}_8 = -\cos \gamma_m (\gamma_m^3 + (m \pi)^2 (2 - \nu) \phi^2 \gamma_m)$$

$$\text{For, } \bar{S}_1 = \frac{\begin{bmatrix} (\bar{e}_9 \bar{e}_{16} - \bar{e}_{12} \bar{e}_{13})(\bar{e}_4 \bar{e}_7 - \bar{e}_3 \bar{e}_8) - \\ (\bar{e}_1 \bar{e}_8 - \bar{e}_5 \bar{e}_4)(\bar{e}_{12} \bar{e}_{15} - \bar{e}_{11} \bar{e}_{16}) \\ (\bar{e}_2 \bar{e}_8 - \bar{e}_6 \bar{e}_4)(\bar{e}_{12} \bar{e}_{15} - \bar{e}_{11} \bar{e}_{16}) - \\ (\bar{e}_{10} \bar{e}_{16} - \bar{e}_{12} \bar{e}_{14})(\bar{e}_4 \bar{e}_7 - \bar{e}_3 \bar{e}_8) \end{bmatrix}}{\begin{bmatrix} (\bar{e}_9 \bar{e}_{14} - \bar{e}_{10} \bar{e}_{13})(\bar{e}_8 \bar{e}_2 - \bar{e}_4 \bar{e}_6) - \\ (\bar{e}_1 \bar{e}_6 - \bar{e}_5 \bar{e}_2)(\bar{e}_{16} \bar{e}_{10} - \bar{e}_{12} \bar{e}_{14}) \\ (\bar{e}_3 \bar{e}_6 - \bar{e}_7 \bar{e}_2)(\bar{e}_{16} \bar{e}_{10} - \bar{e}_{12} \bar{e}_{14}) - \\ (\bar{e}_{11} \bar{e}_{14} - \bar{e}_{10} \bar{e}_{15})(\bar{e}_8 \bar{e}_2 - \bar{e}_4 \bar{e}_6) \end{bmatrix}}$$

$$\bar{S}_2 = \frac{\begin{bmatrix} (\bar{e}_9 \bar{e}_{14} - \bar{e}_{10} \bar{e}_{13})(\bar{e}_8 \bar{e}_2 - \bar{e}_4 \bar{e}_6) - \\ (\bar{e}_1 \bar{e}_6 - \bar{e}_5 \bar{e}_2)(\bar{e}_{16} \bar{e}_{10} - \bar{e}_{12} \bar{e}_{14}) \\ (\bar{e}_3 \bar{e}_6 - \bar{e}_7 \bar{e}_2)(\bar{e}_{16} \bar{e}_{10} - \bar{e}_{12} \bar{e}_{14}) - \\ (\bar{e}_{11} \bar{e}_{14} - \bar{e}_{10} \bar{e}_{15})(\bar{e}_8 \bar{e}_2 - \bar{e}_4 \bar{e}_6) \end{bmatrix}}{\begin{bmatrix} (\bar{e}_9 \bar{e}_{15} - \bar{e}_{11} \bar{e}_{13})(\bar{e}_6 \bar{e}_3 - \bar{e}_2 \bar{e}_7) - \\ (\bar{e}_1 \bar{e}_7 - \bar{e}_5 \bar{e}_3)(\bar{e}_{14} \bar{e}_{11} - \bar{e}_{10} \bar{e}_{15}) \\ (\bar{e}_4 \bar{e}_7 - \bar{e}_3 \bar{e}_8)(\bar{e}_{14} \bar{e}_{11} - \bar{e}_{10} \bar{e}_{15}) - \\ (\bar{e}_{12} \bar{e}_{15} - \bar{e}_{11} \bar{e}_{16})(\bar{e}_6 \bar{e}_3 - \bar{e}_2 \bar{e}_7) \end{bmatrix}}$$

$$\bar{S}_3 = \frac{\begin{bmatrix} (\bar{e}_9 \bar{e}_{15} - \bar{e}_{11} \bar{e}_{13})(\bar{e}_6 \bar{e}_3 - \bar{e}_2 \bar{e}_7) - \\ (\bar{e}_1 \bar{e}_7 - \bar{e}_5 \bar{e}_3)(\bar{e}_{14} \bar{e}_{11} - \bar{e}_{10} \bar{e}_{15}) \\ (\bar{e}_4 \bar{e}_7 - \bar{e}_3 \bar{e}_8)(\bar{e}_{14} \bar{e}_{11} - \bar{e}_{10} \bar{e}_{15}) - \\ (\bar{e}_{12} \bar{e}_{15} - \bar{e}_{11} \bar{e}_{16})(\bar{e}_6 \bar{e}_3 - \bar{e}_2 \bar{e}_7) \end{bmatrix}}{\begin{bmatrix} (\bar{e}_9 \bar{e}_{15} - \bar{e}_{11} \bar{e}_{13})(\bar{e}_6 \bar{e}_3 - \bar{e}_2 \bar{e}_7) - \\ (\bar{e}_1 \bar{e}_7 - \bar{e}_5 \bar{e}_3)(\bar{e}_{14} \bar{e}_{11} - \bar{e}_{10} \bar{e}_{15}) \\ (\bar{e}_4 \bar{e}_7 - \bar{e}_3 \bar{e}_8)(\bar{e}_{14} \bar{e}_{11} - \bar{e}_{10} \bar{e}_{15}) - \\ (\bar{e}_{12} \bar{e}_{15} - \bar{e}_{11} \bar{e}_{16})(\bar{e}_6 \bar{e}_3 - \bar{e}_2 \bar{e}_7) \end{bmatrix}}$$

$$\text{For, } \bar{e}_1 = \left(\frac{\sinh(\beta_m \eta_o) + (\beta_m^3 - (m \pi)^2 (2 - \nu) \phi^2 \beta_m)}{(\gamma_m^3 + (m \pi)^2 (2 - \nu) \phi^2 \gamma_m)} \sin(\gamma_m \eta_o) \right)$$

$$\bar{e}_2 = \left(\cos(\gamma_m \eta_o) + \frac{(\gamma_m^2 + (m \pi)^2 \nu \phi^2)}{(\beta_m^2 - (m \pi)^2 \nu \phi^2)} \cosh(\beta_m \eta_o) \right)$$

$$\bar{e}_3 = -\left(\frac{\sinh(\beta_m \eta_o) + (\beta_m^3 - (m \pi)^2 (2 - \nu) \phi^2 \beta_m)}{(\gamma_m^3 + (m \pi)^2 (2 - \nu) \phi^2 \gamma_m)} \sin(\gamma_m \eta_o) \right)$$

$$\bar{e}_4 = -\left(\frac{\cos(\gamma_m \eta_o) + (\gamma_m^2 + (m \pi)^2 \nu \phi^2)}{(\beta_m^2 - (m \pi)^2 \nu \phi^2)} \cosh(\beta_m \eta_o) \right)$$

$$\bar{e}_5 = \left[\frac{\sinh(\beta_m \eta_o) (\beta_m^2 - (m \pi)^2 \nu \phi^2) - (\beta_m^3 - (m \pi)^2 (2 - \nu) \phi^2 \beta_m)}{(\gamma_m^3 + (m \pi)^2 (2 - \nu) \phi^2 \gamma_m)} \sin(\gamma_m \eta_o) (\gamma_m^2 + (m \pi)^2 \nu \phi^2) \right]$$

$$\bar{e}_6 = \left[-\cos(\gamma_m \eta_o) (\gamma_m^2 + (m \pi)^2 \nu \phi^2) + (\gamma_m^2 + (m \pi)^2 \nu \phi^2) \cosh(\beta_m \eta_o) \right]$$

$$\bar{e}_7 = -\left[\frac{\sinh(\beta_m \eta_o) (\beta_m^2 - (m \pi)^2 \nu \phi^2) + (\beta_m^3 - (m \pi)^2 (2 - \nu) \phi^2 \beta_m)}{(\gamma_m^3 + (m \pi)^2 (2 - \nu) \phi^2 \gamma_m)} \sin(\gamma_m \eta_o) (\gamma_m^2 + (m \pi)^2 \nu \phi^2) \right]$$

$$\begin{aligned} \bar{e}_8 &= - \begin{bmatrix} -\cos(\gamma_m \eta_o) (\gamma_m^2 + (m \pi)^2 \nu \phi^2) + \\ \bar{d}_{12} \cosh(\beta_m \eta_o) (\beta_m^2 - (m \pi)^2 \nu \phi^2) - \\ \bar{d}_{10} \sin(\gamma_m \eta_o) (\gamma_m^2 + (m \pi)^2 \nu \phi^2) \end{bmatrix} \\ \bar{e}_9 &= \begin{bmatrix} \cosh(\beta_m \eta_o) (\beta_m^3 - (m \pi)^2 (2 - \nu) \phi^2 \beta_m) - \\ (\beta_m^3 - (m \pi)^2 (2 - \nu) \phi^2 \beta_m) \cos(\gamma_m \eta_o) \end{bmatrix} \\ \bar{e}_{10} &= \begin{bmatrix} \sin(\gamma_m \eta_o) (\gamma_m^3 + (m \pi)^2 (2 - \nu) \phi^2 \gamma_m) + \\ \left[\left(\frac{(\gamma_m^2 + (m \pi)^2 \nu \phi^2)}{(\beta_m^2 - (m \pi)^2 \nu \phi^2)} \sinh(\beta_m \eta_o) \right) * \right. \\ \left. \left(\frac{\beta_m^3 - (m \pi)^2 (2 - \nu) \phi^2 \beta_m}{(m \pi)^2 (2 - \nu) \phi^2 \beta_m} \right) \right] \end{bmatrix} \\ \bar{e}_{11} &= - \begin{bmatrix} \cosh(\beta_m \eta_o) \left((m \pi)^2 (2 - \nu) \phi^2 \beta_m \right) + \\ \beta_m^3 - \\ \bar{d}_{11} \sinh(\beta_m \eta_o) \left((m \pi)^2 (2 - \nu) \phi^2 \beta_m \right) - \\ \bar{d}_9 \cos(\gamma_m \eta_o) (\gamma_m^3 + (m \pi)^2 (2 - \nu) \phi^2 \gamma_m) \end{bmatrix} \\ \bar{e}_{12} &= - \begin{bmatrix} \sin(\gamma_m \eta_o) (\gamma_m^3 + (m \pi)^2 (2 - \nu) \phi^2 \gamma_m) + \\ \bar{d}_{12} \sinh(\beta_m \eta_o) \left((m \pi)^2 (2 - \nu) \phi^2 \beta_m \right) - \\ \beta_m^3 - \\ \bar{d}_{10} \cos(\gamma_m \eta_o) (\gamma_m^3 + (m \pi)^2 (2 - \nu) \phi^2 \gamma_m) \end{bmatrix} \\ \bar{e}_{13} &= \begin{bmatrix} \beta_m \cosh(\beta_m \eta_o) + \\ \frac{(\beta_m^3 - (m \pi)^2 (2 - \nu) \phi^2 \beta_m)}{(\gamma_m^2 + (m \pi)^2 (2 - \nu) \phi^2 \gamma_m)} \gamma_m \cos(\gamma_m \eta_o) - \\ f_e(\zeta) \left[\begin{bmatrix} \sinh(\beta_m \eta_o) (\beta_m^2 - (m \pi)^2 \nu \phi^2) - \\ \frac{(\beta_m^3 - (m \pi)^2 (2 - \nu) \phi^2 \beta_m)}{(\gamma_m^2 + (m \pi)^2 (2 - \nu) \phi^2 \gamma_m)} * \\ \sin(\gamma_m \eta_o) (\gamma_m^2 + (m \pi)^2 \nu \phi^2) \end{bmatrix} \right] \end{bmatrix} \\ \bar{e}_{14} &= \begin{bmatrix} -\gamma_m \sin(\gamma_m \eta_o) + \\ \frac{(\gamma_m^2 + (m \pi)^2 \nu \phi^2)}{(\beta_m^2 - (m \pi)^2 \nu \phi^2)} \beta_m \sinh(\beta_m \eta_o) - \\ f_e(\zeta) \left[\begin{bmatrix} -\cos(\gamma_m \eta_o) (\gamma_m^2 + (m \pi)^2 \nu \phi^2) + \\ (\gamma_m^2 + (m \pi)^2 \nu \phi^2) \cosh(\beta_m \eta_o) \end{bmatrix} \right] \end{bmatrix} \\ \bar{e}_{15} &= - \begin{bmatrix} \beta_m \cosh(\beta_m \eta_o) + \\ \bar{d}_{11} \beta_m \sinh(\beta_m \eta_o) + \\ \bar{d}_9 \gamma_m \cos(\gamma_m \eta_o) \end{bmatrix} \\ \bar{e}_{16} &= - \begin{bmatrix} -\gamma_m \sin(\gamma_m \eta_o) + \\ \bar{d}_{12} \beta_m \sinh(\beta_m \eta_o) + \\ \bar{d}_{10} \gamma_m \cos(\gamma_m \eta_o) \end{bmatrix} \end{aligned}$$

And the value of λ can be evaluated from the characteristics equations, as,

$$\begin{bmatrix} \bar{e}_1 & \bar{e}_2 & \bar{e}_3 & \bar{e}_4 \\ \bar{e}_5 & \bar{e}_6 & \bar{e}_7 & \bar{e}_8 \\ \bar{e}_9 & \bar{e}_{10} & \bar{e}_{11} & \bar{e}_{12} \\ \bar{e}_{13} & \bar{e}_{14} & \bar{e}_{15} & \bar{e}_{16} \end{bmatrix} = 0 \quad (27)$$

For vibration analysis of the plate having a crack with a finite length, relation Eqs. (22), (24), and (26) can be expanded as a double Fourier series in the domain $(-1 \leq \eta \leq 1)$ and $(-1 \leq \zeta \leq 1)$.

Then, by substitution $(W(\zeta, \eta))$ into Eq. (34), then by using orthogonal method, **A. Jeffrey (2002)**, by pre multiplying the result by $(W(\zeta, \eta))$ and integral with ζ, η for $0 \leq \zeta \leq 1, 0 \leq \eta \leq 1$, get the natural frequency of rectangular plate with crack effect at any location and size of crack in ζ direction, as,

$$\frac{\partial^2 w(t)}{\partial t^2} + \omega_p^2 w(t) = 0 \tag{35}$$

where, ω_p^2 is the natural frequency of plate with crack effect defined as,

$$\omega_p^2 = \frac{\int_0^1 \int_0^1 \left(\phi^4 \left(\frac{E_1}{1-\nu_{12}\nu_{21}} \right) \frac{\partial^4 W(\zeta, \eta)}{\partial \zeta^4} + \left[\frac{\nu_{21} E_1}{1-\nu_{12}\nu_{21}} \right]^+ \left[\frac{\nu_{12} E_2}{1-\nu_{12}\nu_{21}} \right] \frac{\partial^4 W(\zeta, \eta)}{\partial \zeta^2 \partial \eta^2} + 4G_{12} \right) d\zeta d\eta}{\frac{12\rho b^4}{H^2} \int_0^1 \int_0^1 (W(\zeta, \eta)W(\zeta, \eta)) d\zeta d\eta} \tag{36}$$

Computer Program

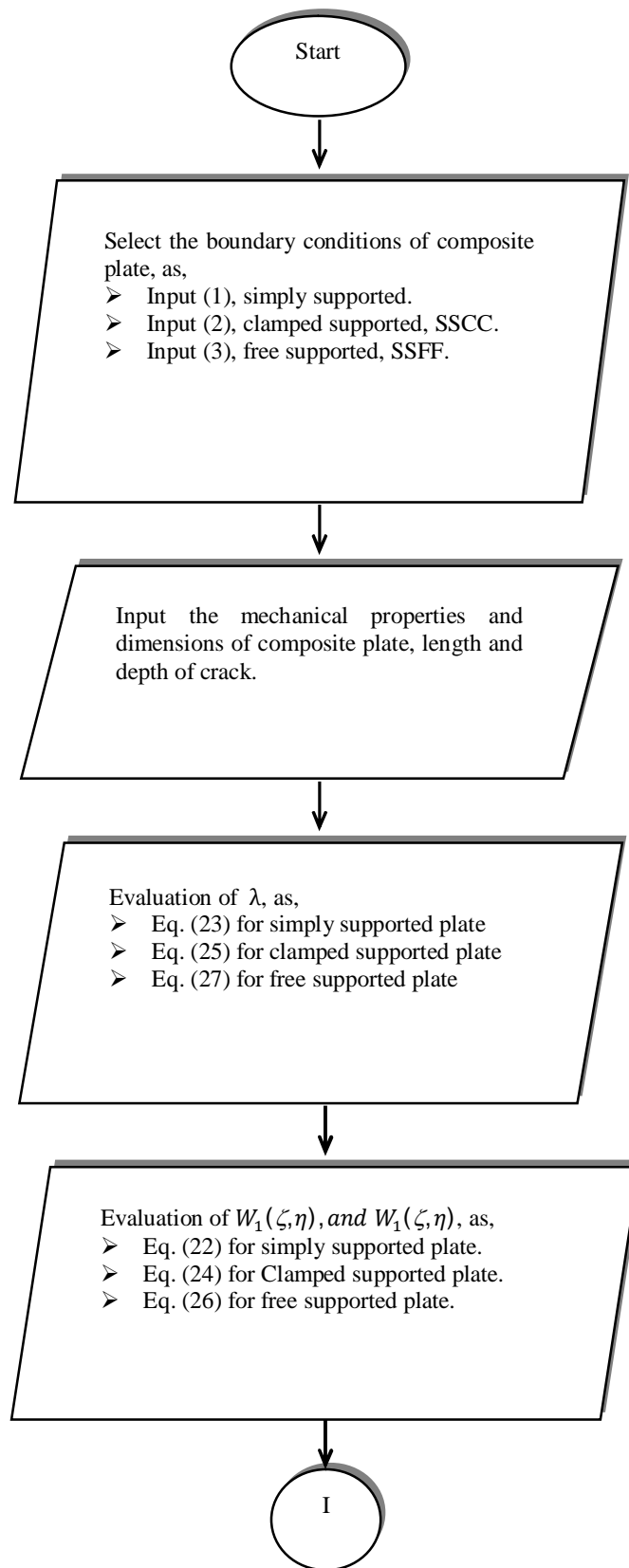
Fig. 2 shows the flow chart for computer program for dynamic analysis of orthotropic composite plate with strength different crack size and location effect. The results are natural frequency of orthotropic composite plate supported as simply supported along edges parallel to crack and other ends as simply, clamped, and free supported of plate, for strength crack, and simply supported plate for oblique crack study. In addition to study the effect of crack size (length and depth), and crack location on the natural frequency of isotropic and orthotropic composite plate.

The program requirement the following input data,

1. Crack information, crack length, crack depth, and position of crack.
2. Plate properties, modulus of elasticity, Poisson ratio and density of plate
3. Dimensions of plates, length of plate, width of plate, and thickness of plate.

And the output of natural frequency get from program are with different parameters as,

- Natural frequency with different crack variable, as,
 1. Natural frequency with different location of crack in ζ -direction.
 2. Natural frequency with different location of crack in η -direction.
 3. Natural frequency with different crack length.
 4. Natural frequency with different crack depth.
- Natural frequency with different plate variable, as,
 1. Natural frequency with different aspect ratio of plate.
 2. Natural frequency with different thickness of plate.
 3. Natural frequency with different boundary conditions of plate, as,
 - a. Simply supported along all edges, SSSS.
 - b. Simply supported along edges ($\zeta=0, 1$) and clamped supported along edges ($\eta=0, 1$), SSCC.
 - c. Simply supported along edges ($\zeta=0, 1$) and free supported along edges ($\eta=0, 1$), SSFF.



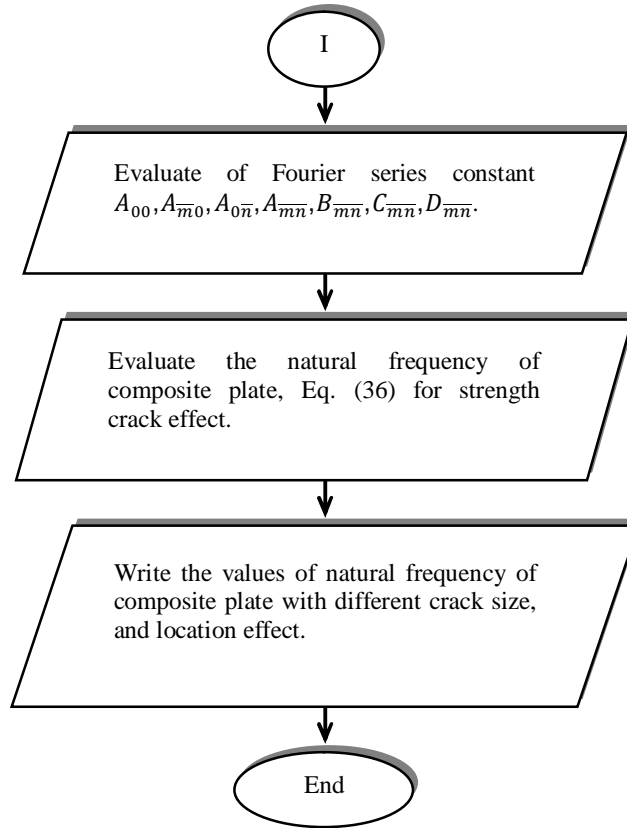


Fig. 2: Flow Chart of Natural Frequency Computer Program of Composite Plate

RESULTS AND DISCUSSIONS

The results are the evaluation of the natural frequency of composite plate types, long and woven composite plate made of polyester resin and glass fiber with ($V_f=30\%$, $G_{\text{glass}}=30$ Gpa, $G_{\text{Polyester}}=1.4$ Gpa, $\nu_{\text{glass}}=0.25$, $\nu_{\text{Polyester}}=0.4$, $E_{\text{glass}}=95$ Gpa, $E_{\text{Polyester}}=3.8$ Gpa, $\rho_{\text{glass}}=2600$ kg/m³, $\rho_{\text{Polyester}}=1350$ kg/m³), with crack effect of plate, included the effect of composite materials types, crack size, crack location, and other parameters of composite plate types. Where the properties of composite plate types and parameters studied are shows in the **Tables 1 and 2**. And, the method studied to evaluated the natural frequency of composite plate types with crack effect are, theoretical study and numerical study, by using ANSYS Program Version 14.

Fig. 3 shown the natural frequency of long composite plate type with aspect ratio (AR=1, 1.5, and 2) for (SSSS, SSCC, and SSFF supported) for composite plate, with different crack position in ζ -direction, for $\eta = 0.5$, $H = 5.5$ mm, $2C = 24$ mm, $\xi = 0.7$, and $V_f = 30\%$. The figure showed that the good agreement between the theoretically and numerical results, where the percentage of discrepancy between the theoretically and numerically results are about (1 to 2%).

Fig. 4 shown the natural frequency of long composite plate with aspect ratio (AR=1, 1.5, and 2) for (SSSS, SSCC, and SSFF supported) for composite plate, with different crack position in η -direction, for $\zeta = 0.5$, $H = 5.5$ mm, $2C = 24$ mm, $\xi = 0.7$, and $V_f = 30\%$. The figures showed that the good agreement between the theoretically and numerical results, where the percentage of discrepancy between the theoretically and numerically results are about (1 to 3.5%).

Table 1: Properties of Composite Materials Types of Composite Plate, M. J. Jweeg et al. (2012)

Properties	Reinforcement Fiber Types (Glass-Polyester)	
	Long Fiber	Woven Fiber
E_1 (Gpa)	31.16	18.25
E_2 (Gpa)	5.34	18.25
G_{12} (Gpa)	1.96	1.96
Density (kg/m^3)	1525	1420
ν_{12}	0.355	0.355

Table 2: Dimensions and Information of Crack and Plate Studied in Theoretical and numerical Study of Vibration Composite Plate

Position of Crack through the ζ -direction (%a)	0.1 to 0.9
Position of Crack through the η -direction (%b)	0.1 to 0.9
Crack Depth h_o (%H)	10%, 30%, 50%, 70%
Crack Length (cm) (%a)	5%, 10%, 15%, 20%
Plate Length, a (cm)	24
Plate Width (cm)	24, 36, 48
Aspect ratio (b/a)	1, 1.5, 2
Plate Thickness (mm)	3.5, 5.5, 9
Boundary Conditions	SSSS, SSCC, SSFF

Fig. 5 shown the effect of the crack position in η -direction on the natural frequency of different composite plate types long, and woven reinforcement fiber), with different aspect ratio (1, 1.5, and 2) and boundary condition of plate as (SSSS, SSCC, and SSFF) for plate thickness $H = 5.5 \text{ mm}$, crack length $2C = 24 \text{ mm}$, crack depth ratio $\xi = 0.7$, middle crack position in ζ -direction $\zeta = 0.5$, volume fraction of reinforcement fiber $\nu_f = 30\%$, and 0° crack angle. From figures shown that the effect of crack position more effect at middle location of plate in ζ -direction. From figures shown that the effect of crack position more effect at middle location of plate in η -direction.

Fig. 6 shown the effect of the crack position in ζ -direction on the natural frequency of different composite plate types (long, and woven reinforcement fiber), with different aspect ratio (1, 1.5, and 2) and boundary condition of plate as (SSSS, SSCC, and SSFF) for plate thickness $H = 5.5 \text{ mm}$, crack length $2C = 24 \text{ mm}$, crack depth ratio $\xi = 0.7$, middle crack position in η -direction $\eta = 0.5$, volume fraction of reinforcement fiber $V_f = 30\%$, and 0° crack angle. From figures shown that the effect of crack position more effect at middle location of plate in ζ -direction.

Fig. 7 shown the effect of the crack length on the natural frequency of different composite plate types (long, and woven fiber), with different aspect ratio (1, 1.5, and 2) and boundary condition of plate as (SSSS, SSCC, and SSFF) for middle crack position in ζ and η -direction $\eta = 0.5, \zeta = 0.5$, plate thickness $H = 5.5 \text{ mm}$, crack depth ratio $\xi = 0.7$, volume fraction of reinforcement fiber $V_f = 30\%$, and 0° crack angle. From figure shown that the natural frequency decreasing with increasing of crack length.

Fig. 8 shown the effect of the crack depth ratio on the natural frequency of different composite plate types (long, and woven fiber), with different aspect ratio (1, 1.5, and 2) and boundary condition of plate as (SSSS, SSCC, and SSFF) for middle crack position in ζ and η -direction $\eta = 0.5, \zeta = 0.5$, plate thickness $H = 5.5 \text{ mm}$, crack length $2C = 24 \text{ mm}$, volume fraction of reinforcement fiber $V_f = 30\%$, and 0° crack angle. From figure shown that the natural frequency decreasing with increasing of depth.

Fig. 9 shown the effect of the plate thickness on the natural frequency of different composite plate types (long, and woven fiber), with different aspect ratio (1, 1.5, and 2) and boundary condition of plate as (SSSS, SSCC, and SSFF) for middle crack position in ζ and η -direction $\eta = 0.5, \zeta = 0.5$, plate crack depth ratio $\xi = 0.7$, crack length $2C = 24 \text{ mm}$, volume fraction of reinforcement fiber $V_f = 30\%$, and 0° crack angle. From figure shown that the natural frequency increasing with increasing of plate thickness.

From **Figs. 5 to 9** shows the following effect of the crack and plate on the natural frequency of plate with crack effect,

Effect of Crack Position (ζ and η -Direction)

The natural frequency of composite plate types decreasing with move crack position near the middle location plate, since the stiffness of plate is decreasing with the moving the crack to the middle plate location, then decreasing of the natural frequency of plate, as shows in **Figs. 5 and 6** with different composite plate types, aspect ratio, boundary condition, and crack orientation effect.

Crack Size Effect (Length and Depth)

The natural frequency of composite plate is decreasing with the increasing of the crack size as length of crack or depth since the crack cause decreasing of the stiffness of plate, then cause decreasing of the natural frequency of plate, as shows in **Figs. 7 and 8** with different composite plate types, aspect ratio, boundary condition, and crack orientation effect.

Plate Thickness Effect

The increasing of plate thickness cause an increasing of the stiffness of plate more than the increasing of plate mass, the increasing of plate thickness cause increase of plate frequency due to increasing of plate stiffness as shown in **Fig. 9** for different composite plate types, boundary conditions, and aspect ratio of plate effect.

Effect of Boundary Condition of Plate

The natural frequency of plate at SSFF more than for SSCC and SSSS since the deflection of plate with SSFF supported more than deflection of plate with SSCC and SSSS and frequency of plate with SSCC condition more than frequency of plate with SSSS, the stiffness of SSFF plate more than for other supported and stiffness of SSCC plate more than for stiffness SSSS plate as shows in **Figs. 5 to 9** for different composite plate types, aspect ratio, crack position, and crack size effect.

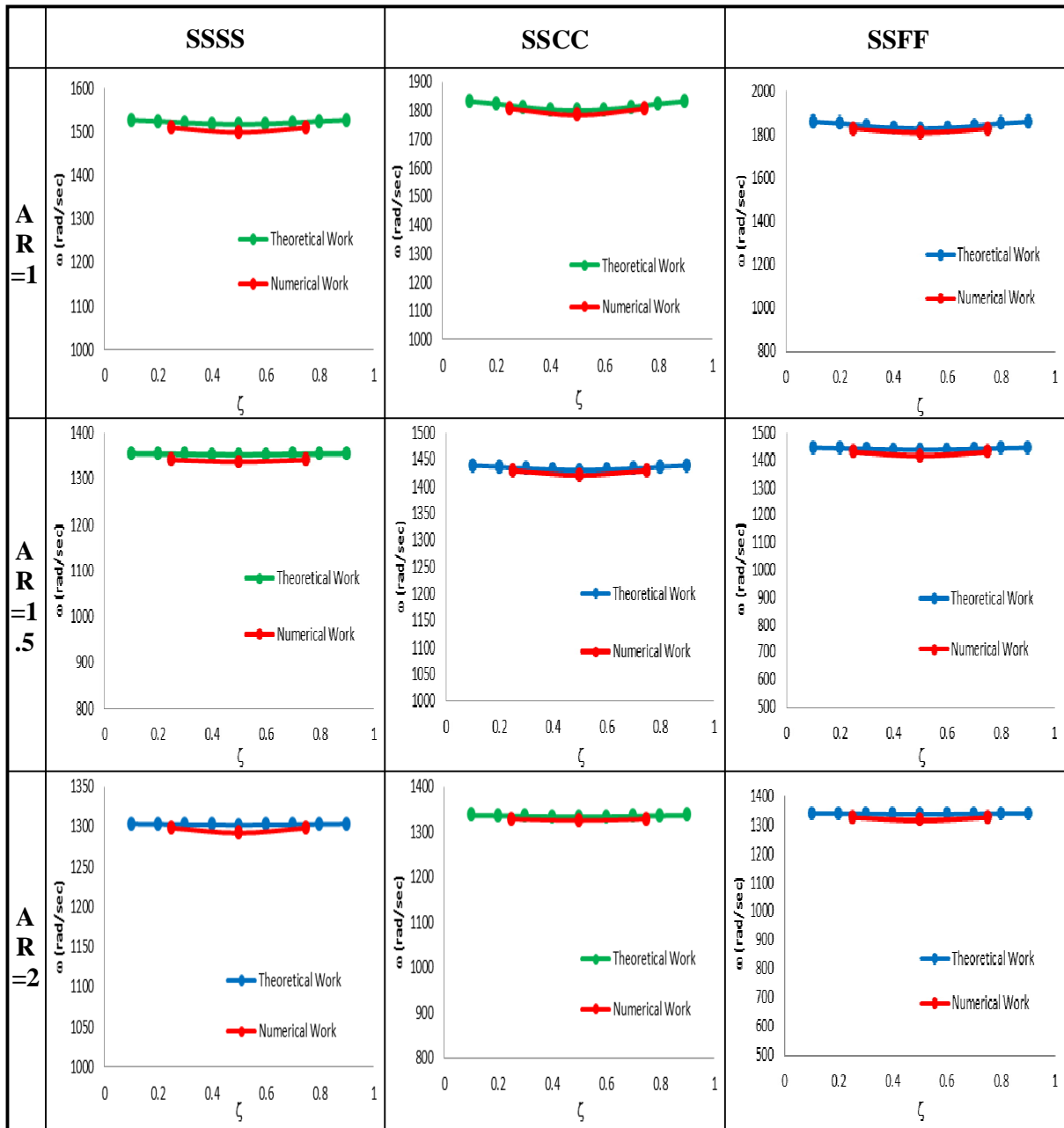


Fig. 3 Compare Between Theoretical and Numerical Work of Natural Frequency for Long Composite Plate with Different Crack Position Effect in ζ -Direction with Different Aspect Ratio and Boundary Condition Plate for, $\eta=0.5$, $2C=24$ mm, $\xi=0.7$

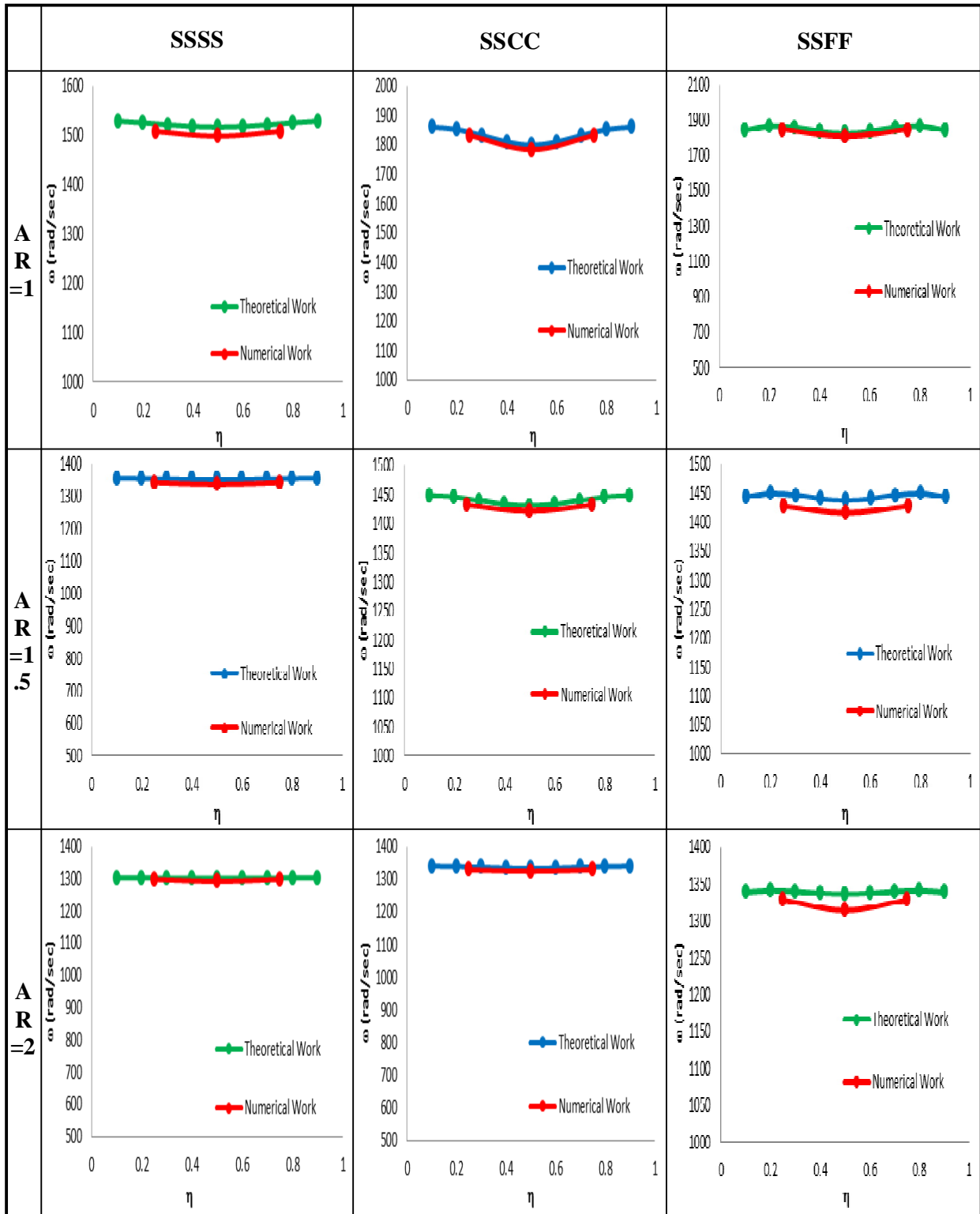


Fig. 4 Compare Between Theoretical and Numerical Work of Natural Frequency for Long Composite Plate with Different Crack Position Effect in η -Direction with Different Aspect Ratio and Boundary Condition Plate for, $\zeta=0.5$, $2C=24$ mm, $\xi=0.7$

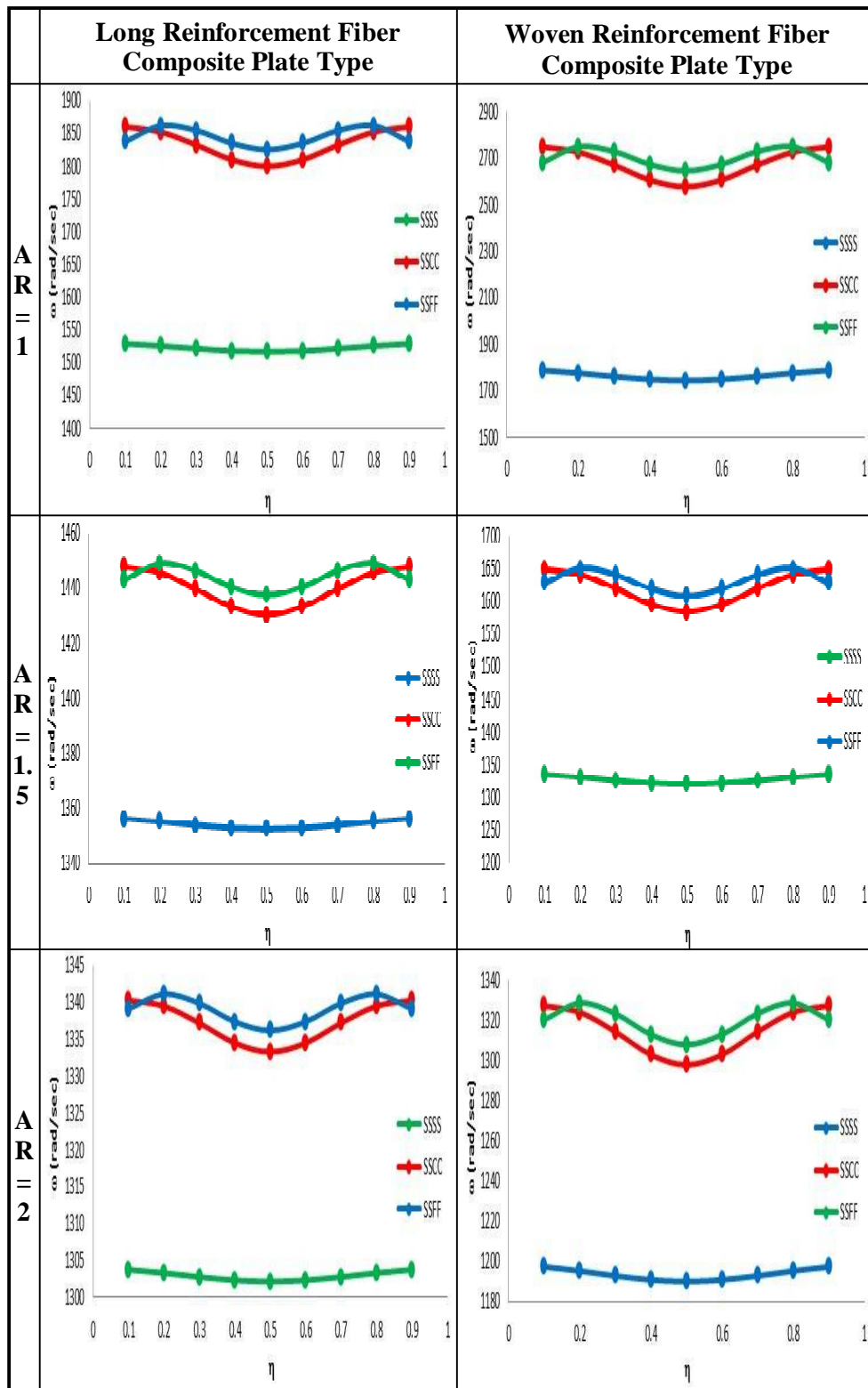


Fig. 5 Natural Frequency (rad/sec) of Orthotropic (Long, Woven) Composite Plate with Different Crack Position in η -Direction Effect with Different Aspect Ratio and Boundary Condition Plate for, $\zeta=0.5$, $\xi=0.7$, $\nabla=30\%$, $H=5.5$ mm, $2C=24$ mm, and 0° Crack Angle

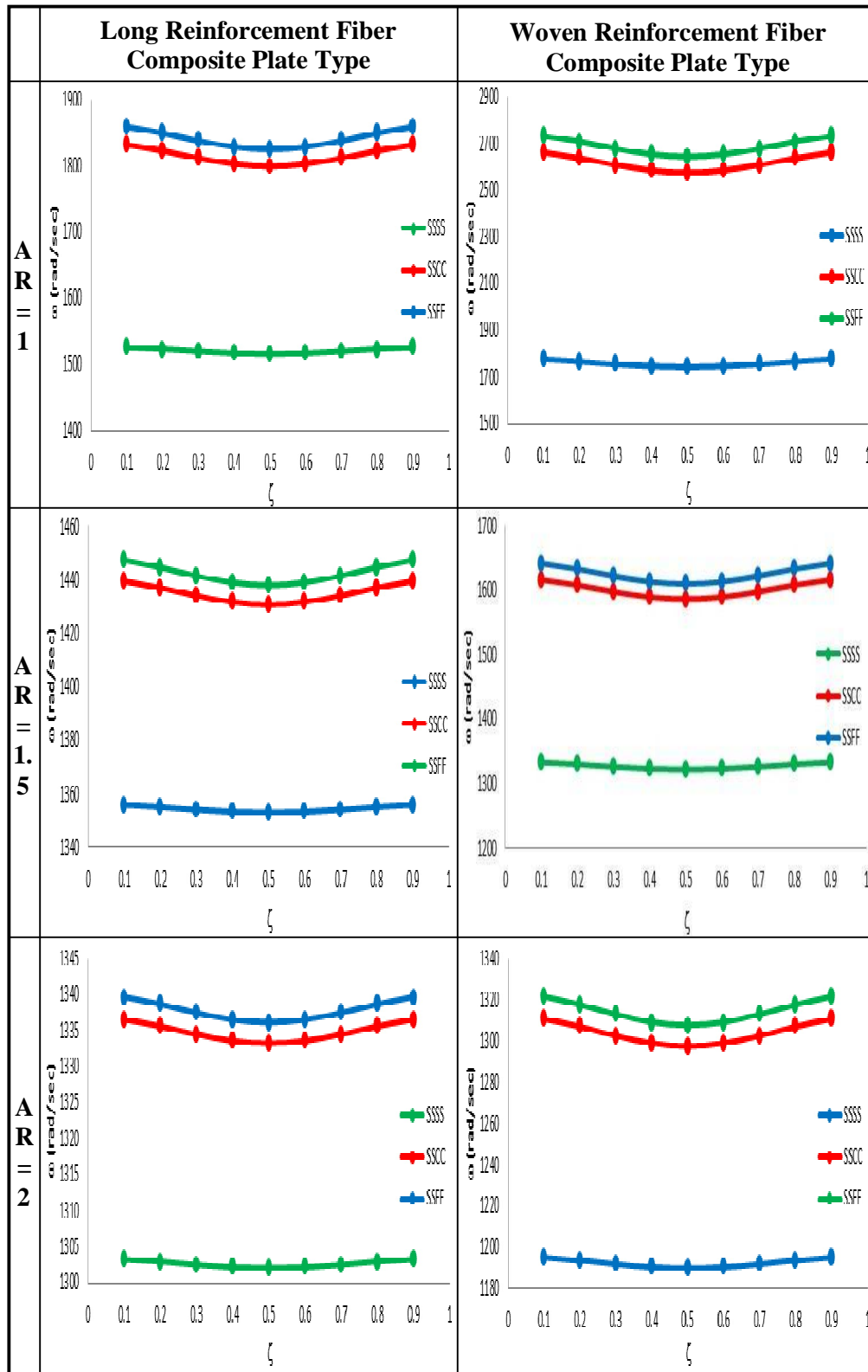


Fig. 6 Natural Frequency (rad/sec) of Orthotropic (Long, Woven) Composite Plate with Different Crack Position in ζ -Direction Effect with Different Aspect Ratio and Boundary Condition Plate for, $\eta=0.5$, $\xi=0.7$, $\nu=30\%$, $H=5.5$ mm, $2C=24$ mm, and 0° Crack Angle

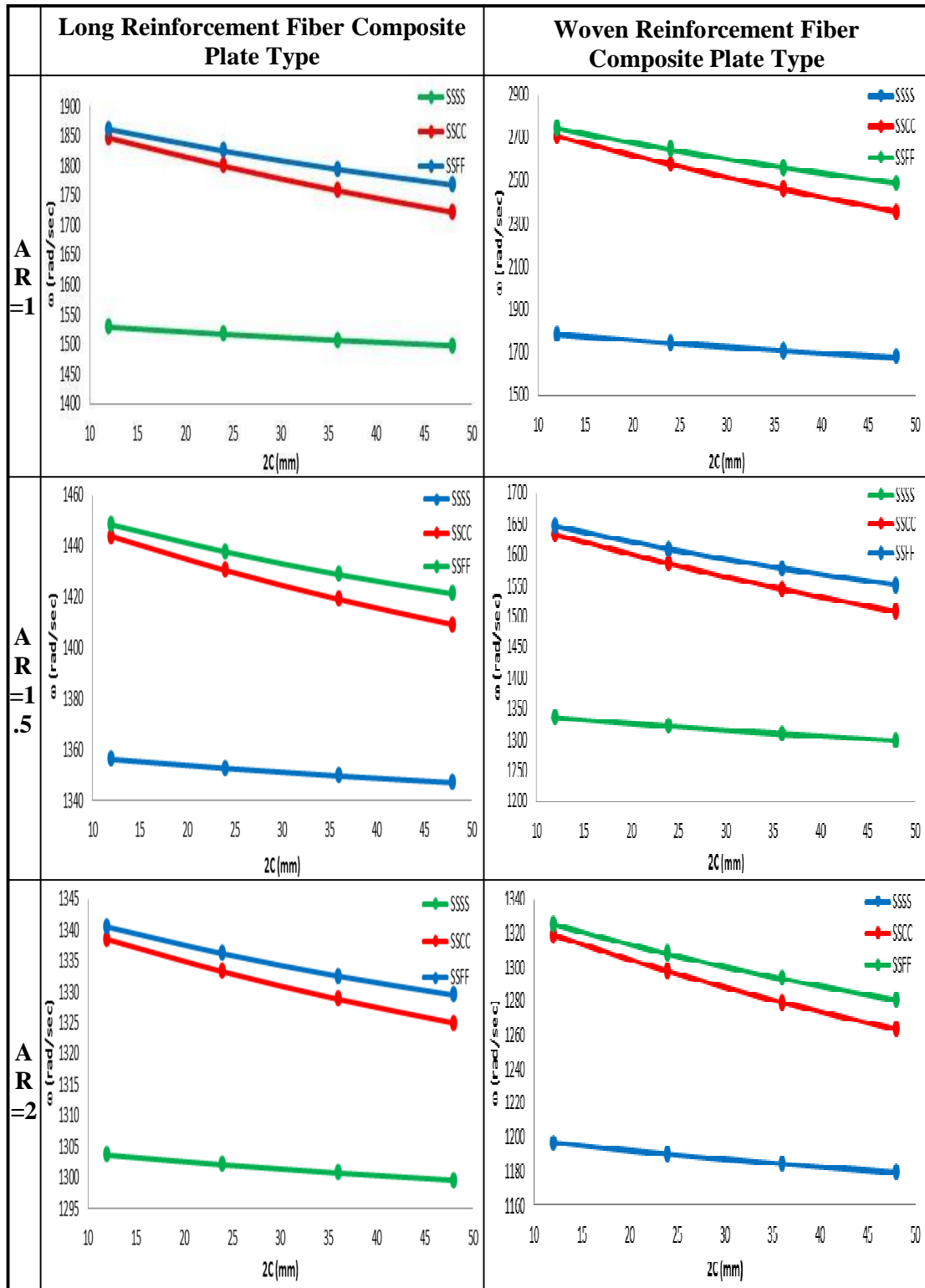


Fig. 7 Natural Frequency (rad/sec) of Orthotropic (Long, Woven) Composite Plate with Different Crack Length Effect with Different Aspect Ratio and Boundary Condition Plate for, $\eta=0.5$, $\zeta=0.5$, $\xi=0.7$, $\nu=30\%$, $H=5.5$ mm, and 0° Crack Angle

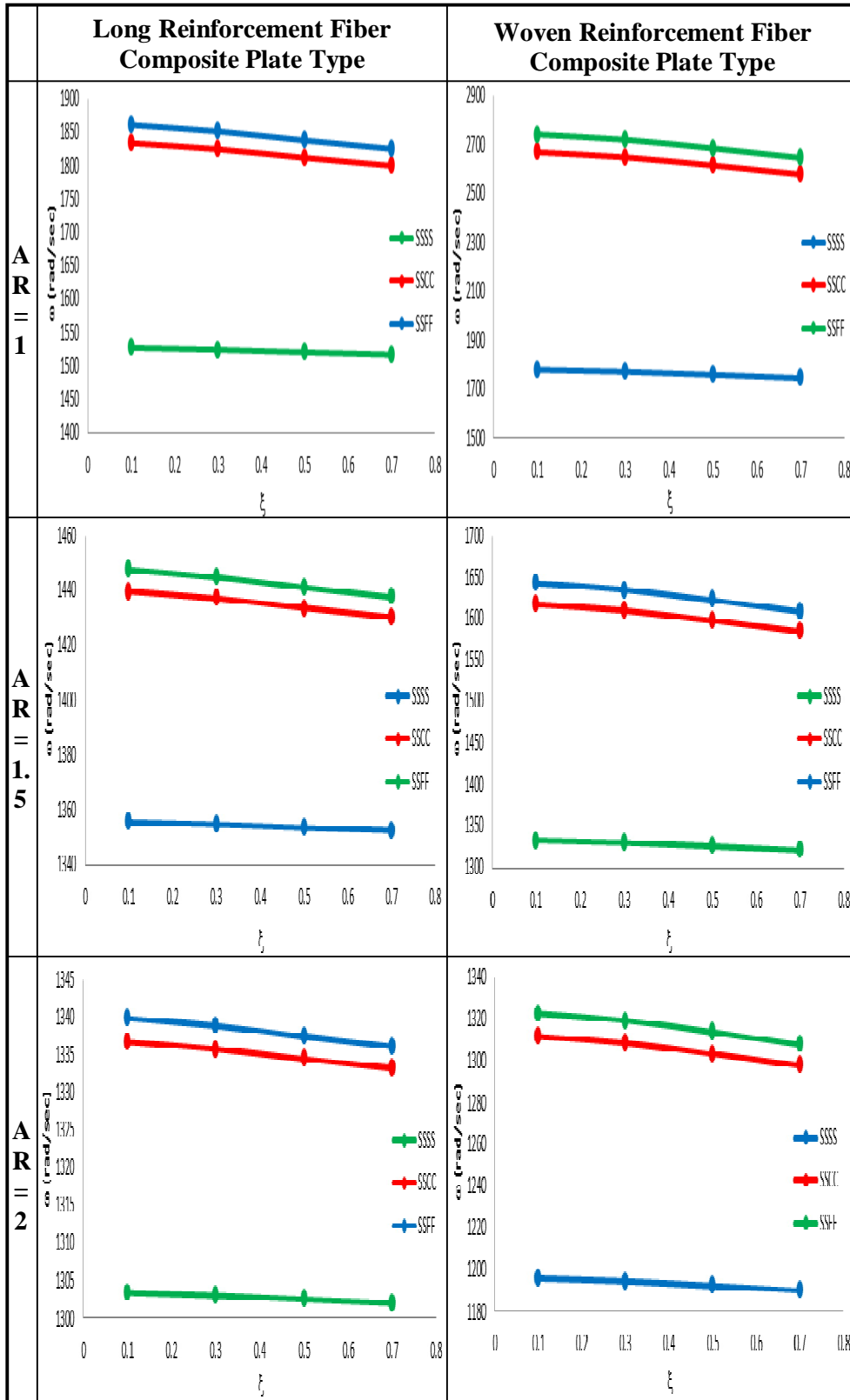


Fig. 8 Natural Frequency (rad/sec) of Orthotropic (Long, Woven) Composite Plate with Different Crack Depth Ratio Effect with Different Aspect Ratio and Boundary Condition Plate for, $\eta=0.5$, $\zeta=0.5$, $2C=24$ mm, $V=30\%$, $H=5.5$ mm, and 0° Crack Angle

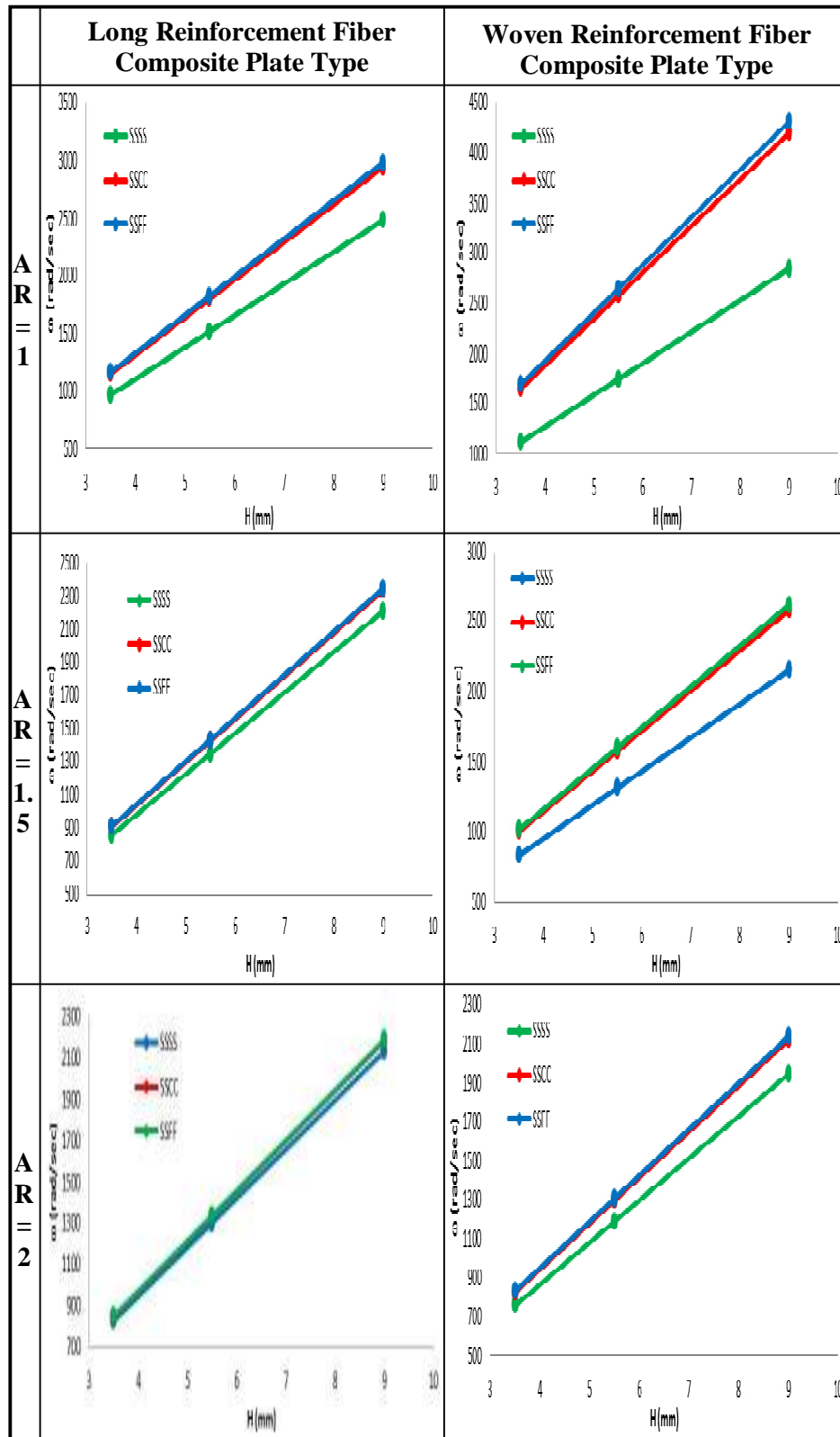


Fig. 9 Natural Frequency (rad/sec) of Orthotropic (Long, Woven) Composite Plate with Different Plate Thickness Effect with Different Aspect Ratio and Boundary Condition Plate for, $\eta=0.5$, $\zeta=0.5$, $\xi=0.7$, $2C=24$ mm, $V=30\%$, and 0° Crack Angle

CONCLUSIONS

The main conclusions of this work for dynamic behavior of orthotropic composite plate types with crack effect are listed below:

1. The suggested analytical solution is a powerful tool to evaluate the natural frequency of orthotropic composite plate with crack, by solution the general differential equations of motion of plate with crack effect by using separation method for differential equation.
2. A comparison made between analytical results from suggested analytical solution study with numerical results from ANSYS program shows a good approximation where the biggest error percentage is about (3.5 %).
3. The position of crack in the plate near the middle of the plate has more effect on the stiffness and natural frequency of plate from the other positions (near to the ends of the plate), i.e. frequency of plate when the crack in the middle position it has a lower frequency of plate with respect to the cracks near to the end position.
4. The crack in the plate has an effect on the stiffness of the plate, this will affect the frequency of the plate. So, with increasing of the crack depth or length (crack size) the stiffness of plate will decreased, this will cause a decreasing the natural frequency of the composite plate.
5. The plate thickness is increases the stiffness of plate and increasing of the natural frequency of plate. And increasing of the aspect ratio decreases of the natural frequency of composite plate.

REFERENCES

1. Ansel C. Ugural 'Stress in Plates and Shells' McGraw-Hill Book Companies, Second Edition,1999.
2. Alan Jeffrey 'Advanced Engineering Mathematics' Harcourt/Academic Press, 2002.
3. Asif Israr 'Vibration Analysis of Cracked Aluminum Plates' Ph. D. Thesis, Engineering Department of Mechanical Engineering, University of Glasgow, 2008.
4. Daniel Gay, Suong V. Hoa and Stephen W. Tsai 'Composite Materials Design and Applications' Book, CRC Press LLC, 2003.
5. Howard Anton, Irl Bivens, and Stephen Davis 'Calculus' Anton Textbooks, Inc, Seventh Edition, (2002).
6. J. R. Rice and N. Levy 'The Part-Through Surface Crack in an Elastic Plate' Journal of Applied Mechanics, Vol. 3, pp. 185-194, 1972.
7. J. S. Rao 'Dynamics of Plates' Narosa Publishing House, 1999.
8. Lei Wang 'Elastic Wave Propagation in Composites and Least-Squares Damage Localization Technique' Master Thesis, Aerospace Engineering, North Carolina State University, 2004.
9. Mana Afshari and Daniel J. Inman 'Continuous Crack Modeling in Piezoelectrically Driven Vibrations of an Euler-Bernoulli Beam' Journal of Vibration and Control, Vol. 18, No. 10, 2012.
10. Muhsin J. Jweeg, Ali S. Hammood, and Muhannad Al-Waily 'Experimental and Theoretical Studies of Mechanical Properties for Reinforcement Fiber Types of Composite Materials' International Journals of Engineering and Sciences, Vol. 12, No. 4, 2012
11. P. Frank Pail and Mannur J. Sundaresan 'Space-Wavenumber and Time-Frequency Analysis for Damage Inspection of Thin-Walled Structures' Structural Health Monitoring, Vol. 11, No. 4, pp. 452-471, 2012.
12. Robert M. Jones 'Mechanics of Composite Materials, Second Edition' Book, Taylor and Francis, 1999.
13. S. E. Khadem and M. Rezaee-a 'Introduction of Modified Comparison Functions for Vibration Analysis of a Rectangular Cracked Plate' Journal of Sound and Vibration, Vol. 236, No. 2, pp. 245-258, 2000

14. S. E. Khadem and M. Rezaee-b 'An Analytical Approach for Obtaining the Location and Depth of an All-Over Part-Through Crack on Externally in-Plane Loaded Rectangular Plate Using Vibration Analysis' *Journal of Sound and Vibration*, Vol. 230, No. 2, pp. 291-308, 2000.
15. Seth S. Kessler, S. Mark Spearing and Constantinos Soutis 'Structural Health Monitoring in Composite Materials Using Lamb Wave Methods' *Technology Laboratory for Advanced Composites*, Department of Aeronautics and Astronautics, Massachusetts Institute of Technology, 2001.